RSC Advances

This is an *Accepted Manuscript*, which has been through the Royal Society of Chemistry peer review process and has been accepted for publication.

Accepted Manuscripts are published online shortly after acceptance, before technical editing, formatting and proof reading. Using this free service, authors can make their results available to the community, in citable form, before we publish the edited article. This *Accepted Manuscript* will be replaced by the edited, formatted and paginated article as soon as this is available.

You can find more information about *Accepted Manuscripts* in the Information for Authors.

Please note that technical editing may introduce minor changes to the text and/or graphics, which may alter content. The journal's standard Terms & Conditions and the Ethical guidelines still apply. In no event shall the Royal Society of Chemistry be held responsible for any errors or omissions in this *Accepted Manuscript* or any consequences arising from the use of any information it contains.

ROYAL SOCIETY OF CHEMISTRY

www.rsc.org/advances

Light-Induced Structural Changes during Early Photo-Intermediates of the Eubacterial Cl^- Pump *Fulvimarina* Rhodopsin Observed by FTIR Difference Spectroscopy

Faisal Hammad Mekky Koua,[*ab] and Hideki Kandori[*ac]

[a] *OptoBioTechnology Research Center, Nagoya Institute of Technology, Showa-ku, 466-8555 Nagoya, Japan.* [b] *Present address: Center for Membrane Biology, Department of Molecular Physiology & Biological Physics, University of Virginia, Charlottesville 22908, Virginia, U. S. A.*

[c] *Department of Frontier Materials, Nagoya Institute of Technology, Showa-ku, 466-8555 Nagoya, Japan*

Corresponding authors:

*fk3p@virginia.edu (F.H.M.K.)

*kandori@nitech.ac.jp (H.K.)

RSC Advances Accepted Manuscript

ABSTRACT: *Fulvimarina pelagi* rhodopsin (FR) is a member of inward eubacterial light-activated Cl^- translocating rhodopsins (ClR) that were found recently in marine bacteria. Here, we present the first detailed low-temperature FTIR difference spectroscopy analyses assisted with static UV-visible spectroscopy on this novel ClR, monitoring its FR_K and $FR_{L\text{-like}}$ ($FR_{L'}$) intermediates at 77 and 220 K, respectively. Light-activated FTIR difference spectra in the fingerprint C–C bands (1290–1040 cm^{-1}) and the hydrogen-out-of-plane (HOOP) wags of the retinal chromophore indicate similar but not identical configurations of the FR_K and $FR_{L'}$, and that the retinal undergoes all-*trans* to 13-*cis* isomerization upon photo-activation similar to other microbial rhodopsins. Further, the analysis of the C=C ethylenic vibrations reveal that FR_K and $FR_{L'}$ states are red-shifted from the unphotolyzed state. Light-induced FTIR difference spectral analyses of the amide I and amide II regions (1700–1560 cm^{-1}), the protein moiety, further suggest that FR undergoes large protein rearrangements during the primary states of photo-activation. In addition, we tentatively assign the bands at 1628 (–)/ 1618 (+) cm^{-1} to the C=N stretching vibrations, that is ~6 (–)/3 (+) cm^{-1} downshifted from its archaeal counterpart halorhodopsin. This assignment reveals that FR undergoes no changes in the C=N stretch upon $FR_{L'}$-formation, suggesting similar hydrogen-bonding and Schiff base environments between FR_K and $FR_{L'}$.

RSC Advances Accepted Manuscript

Introduction

Light-activated ion pumps, known as microbial rhodopsins, are a family of small hepta-helical transmembrane proteins of about 25 kDa that were found predominantly in the halophilic archaeal consortia of marine environments.[1] Additionally, later culture-independent and wide metagenomics approaches identified a high prevalence of rhodopsin homologs in a wide range of bacteria, algae, and fungi.[1,2] These rhodopsins include light-activated outward proton pumps (bacteriorhodopsin, BR;[3] proteorhodopsin;[4] and xanthorhodopsin, XR),[5] light-activated anion pumps (halorhodopsins (HR), N*p*HR; H*s*HR),[6,7] light-activated Na^+ pump (*Krokinobacter eikastus* rhodopsin, KR2; and *Gillisia limnaea* rhodopsin),[8,9] light-activated signal transducers (sensory rhodopsins, SR),[10] and light-gated ion channels (channelrhodopsins, ChR),[11,12] photoreceptors found in eyespots (*stigma*) of green algae. Due to their stability and structural simplicity, microbial rhodopsins have been utilized as model systems in a diverse range of applications and have contributed significantly to our understanding of ion translocations, membrane biology, and bioenergetics.[1,2] In the last decade, microbial rhodopsins have become especially important for their contribution and discovery as transformative biomolecules in the optogenetics field.[1] They have become important players in the study of complex biological processes, such as those related to neurological disorders, *e.g.*, Parkinson's disease.[13] Among the most common rhodopsins used so far in optogenetics are ChR2, HR, and AR3;[13] however, no eubacterial light-activated rhodopsins have been employed in optogenetics until very recently, when KR2[14] was reported to exhibit *in vivo* inhibition to neural activity of the nematode *Caenorhabditis elegans* due to hyperpolarization upon illumination with green light. This is considered to be advantageous over HR[15] and AR-3[16] as an inhibitory optogenetics tool.

Recently, a new group of microbial rhodopsins from marine flavobacteria was identified capable of anion translocation upon photo-activation.[17] Continuing the efforts for discovering new and promising optogenetics tools, we have recently reported the first detailed spectroscopic studies of the eubacterial light-activated Cl^- pump from the marine flavobacterium *Fulvimarina pelagi*: *Fulvimarina* rhodopsin (FR).[18] FR, as a prototypical microbial rhodopsin, hosts an all-*trans* retinal as a chromophore in the dark-stable state (unphotolyzed) that covalently linked to a conserved lysine residue (K246), forming the retinylidene Schiff base (RSB) (Fig. 1 and Fig.

RSC Advances Accepted Manuscript

S1).[18] The retinal chromophore in microbial rhodopsins undergoes photo-isomerization from all-*trans* to 13-*cis* configuration upon light-illumination in the initial events of photo-activation, followed by large conformational changes and rearrangements in the protein secondary structure in subsequent photolyzed states to enable inward or outward ion translocation.[1]

FR, as a eubacterial Cl^- pumping rhodopsin (ClR), is evolutionarily distant from its functional archaeal homologs (*e.g.*, N*p*HR shares only a 23% sequence identity) compared with XR (34%) or KR2 (33%), suggesting that they are evolutionarily distinct and evolved independently (Fig. S1).[17,18] Moreover, the characteristic motif crucial for ion translocation in FR, an NTQ motif formed by residues N110, T114 and Q121, which corresponds to a DTD motif in BR, is different from that of HR, a TSA motif (Fig. 1a).[18,19] FR has been shown to bind Cl^- weakly with ~8× lower affinity (K_d = 80 mM Cl^-) compared to HR (K_d = 3 mM). FR has also shown an obvious anion size dependency, as reported previously with λ_{max} = 518 nm for Cl^- that is red-shifted in larger anions: $Cl^- < Br^- < NO_3^- < I^-$.[18] These data indicate a similar binding mechanism between FR and HR for Cl^- near the retinal Schiff base exerting a spectral-blue shift, although a lack of structural information for FR makes it unclear how Cl^- is bound and translocated.

The FR photocycle is similar to that of archaeal ClR, *e.g.*, N*p*HR, suggesting a common mechanism for Cl^- transport in ClR family.[18,20] Both ClR systems possess multiple L-intermediate states exhibiting similar λ_{max} at ~ 525 nm, but in FR, the L-intermediate is red-shifted (~7 nm; 0.04 eV), whereas it is clearly blue-shifted ($\Delta\lambda$ = 50 nm) in N*p*HR from the unphotolyzed state (λ_{max} = 576 nm). Moreover, both systems lack the L-intermediate in the absence of Cl^-, implying that formation of L-intermediate(s) is a prerequisite for anion translocation in ClR. Similar to HR, FR does not have an M-intermediate, characteristic of a deprotonated Schiff base.[18] The apparent disparity between FR and HR, however, is that all of the photo-intermediates (K, L, and O) in FR are red-shifted,[18] whereas L-state is an obvious blue-shifted photo-intermediate in HR.[21] In FR, the K-intermediate decays to subsequent states in a μs regime to L, which is found in equilibria with K and O (K/L and L/O), and disappears in the absence of anions similar to HR.[18] Despite these similarities, the exact mechanism by which FR transports Cl^- is unclear; thus, more structural information is urgently needed to clearly dissect the mechanistic basis of Cl^- translocation. In HR, early photo-intermediate states K, L_a and L_b can be trapped and measured by IR difference spectroscopy at low-temperatures 77 K, 170 K and

RSC Advances Accepted Manuscript

250 K, respectively.[22] These photo-intermediates can be distinguished by their ethylenic modes which is expected to accompanying the shift in the absorption maximum as K is red-shifted, whereas $L_{a/b}$ is a blue-shifted intermediate.[20] In contrast, the early photo-intermediates in FR are all red-shifted, which adds more complexity to the low-temperature trapping by IR spectroscopy, thus we relied mainly on the hydrogen-out-of-plane (HOOP) modes, whose positive band has been shown to lose intensity upon L-formation in HR making it a reliable indicator for K-intermediate.[23] In addition, the intensity increase at the positive band in amide II region (~1556 cm^{-1}) with contribution from the retinal ethylenic modes, and the RSB C=N-H^+ stretch are also principal features for K-decay and L-formation.[23-25] Thus, FTIR-difference spectroscopy has been an effective tool to study retinal proteins for its high sensitivity to the perturbations of the RSB (*e.g.*, N–H/D and $–C_{15}=N–$ stretches) and the hydrogen-bonding changes in the chromophore's vicinity. Therefore, FTIR difference spectroscopy can provide valuable information pertaining to the conformational changes in both the retinal binding pockets and the protein moiety that are associated with ion translocation in retinal proteins.[26,27]

Experimental Section

Expression and purification of functional FR

A gene encoding a light-driven chloride ion pump from *Fulvimarina pelagi* was optimized for expression in the *E. coli* C41 (DE3) strain and synthesized accordingly (Eurofins Genomics Inc.). The synthesized FR gene was sub-cloned into the pET-modified vector for expressing the full length FR protein tagged with 6× His in the C-terminal region. The *E. coli* C41(DE3) strain was induced with 1 mM isopropyl β-D-thiogalactopyranoside (IPTG) for 4 hours at 37°C. The FR protein was purified as reported previously.[18] The purified protein in elution buffer (containing 30 mM MES-KOH, pH 6.15, 0.5 M NaCl, 0.5 M imidazole, and 0.05% β-DDM) was dialyzed against a buffer containing 50 mM Tris-HCl, pH 8.0, 100 mM NaCl, and 0.03% β-DDM then concentrated using an Amicon Ultra-15 centrifugal filter (30K) from Millipore. The quality of the sample was evaluated using a UV-visible spectrophotometer (UV-2400PC, Shimadzu, Japan). Typical absorption spectra for FR in salt-free and NaCl-containing solution are shown in Fig. S2.

Reconstitution of FR into DOPC proteoliposomes

RSC Advances Accepted Manuscript

For reconstitution, a 1,2-dioleoyl-*sn*-glycero-3-phosphocholine (DOPC) (*E. coli* polar lipids, Avanti Polar Lipids) stored in chloroform was used. The DOPC was air-dried and suspended in a reconstitution buffer composed of 50 mM Tris-HCl, pH 8.0 and 300 mM NaCl supplemented with 0.02% β-DDM. The β-DDM-solubilized FR was mixed with DOPC in 1:20 protein to lipid molar ratio and kept at ambient temperature for 1 h with gentle agitation. About 0.1–0.2 mg Bio-Beads was added to the mixture and incubated overnight at 4 ºC with gentle agitation. The mixture was filtered to remove the Bio-Beads and pure FR liposomes were stored at 4ºC until used.

UV-visible absorption spectroscopy

UV-visible absorption spectra were recorded for a β-DDM solubilized FR solution at ambient temperature in a buffer containing 50 mM Tris-HCl, pH 8.0, and 0.0, 250 or 600 mM NaCl in 1 cm quartz cuvettes using a UV-2400PC UV-Vis spectrophotometer (Shimadzu, Japan). For DOPC-reconstituted FR, H_2O hydrated films prepared in a similar way to that used for FTIR spectroscopy (see next section) were loaded into a UV-visible spectrophotometer (V-550 JASCO, Japan) equipped with a cryostat sample holder (OptistatND, Oxford Instruments). UV-visible absorption spectra were recorded at different temperatures: 293 K, 220 K, and 77 K, before and after illumination with a 1 kW halogen tungsten light source for 2 min using a 520 nm interference filter. For measurements, the spectrophotometer was connected with an integrating sphere to decrease light scattering artefacts.

Light-induced Fourier transform infrared (FTIR) difference spectroscopy

For FTIR measurements, the FR liposomes were washed several times (4–5 resuspension) with a buffer containing 2 mM Tris-HCl, pH 8.0 and 5 mM NaCl and finally resuspended with the same buffer to ~ 0.2 OD/mL. To prepare a film of FR liposomes, 80 µL of the sample was dropped onto an 18 mm diameter BaF_2 window and dried gently for ~1 h using a vacuum desiccator jar. After dehydration, the films were rehydrated with 1–2 µL of H_2O (20% w/v glycerol) or deuterium oxide (D_2O) and covered immediately with another BaF_2 window assisted with rubber O-ring spacers. The hydrations with H_2O or D_2O were optimized to be below 1.0 absorbance unit as indicated in Fig. S3, a typical IR absorption spectrum of a 1 µL D_2O hydrated film. The salt concentration on a dried film was previously estimated to increase by a factor of ~100,[28] and we pre-estimated the concentration dependency in the UV-visible region. From the UV-visible

RSC Advances Accepted Manuscript

absorption spectra recorded at different concentrations in solution, as shown in Fig. S2, we deduced that the hydrated film NaCl concentration is between 250–600 mM, which corresponds to λ_{max} = 520–525 nm; thus a 520 nm interference filter (K-52) was chosen for illumination. Note that λ_{max} obtained from hydrated film measured at 77 K and 220 K lies within this range (Fig. 3). FTIR measurements were recorded at 77 K and 220 K for FR_K-minus-FR and $FR_{L'}$-minus-FR, respectively. It is generally accepted that at 77 K, most of the photoproducts are from the K-intermediate, while some reports suggest a contribution of other K-like states (K_0, K_E and K_L) but not an L-intermediate.[29] On the other hand, the L-intermediate state of microbial rhodopsins such as BR, N*p*HR and PR can be trapped at 170–200 K or higher; we thus attributed the spectral changes upon heating up to 220 K to the decay of the K-intermediate to K/L and/or L/O intermediate and termed the light-induced FTIR difference spectra at 220 K as an L-like intermediate ($FR_{L'}$) since this state was found in quasi-equilibria with K- and O-intermediates. Note that the lowest temperature used to trap an L-state is 170 K for BR.[30] Films were mounted into a Bio-Rad FTS-40K spectrometer (Agilent Technology) equipped with an Oxford DN-1704 cryostat connected to an Oxford ITC-4 temperature controller. Light-minus-dark measurements were conducted as reported previously for KR2.[31] In brief, a 30-min dark adapted hydrated film was measured first before illumination, followed by illuminating the film for 2 min using a 520 nm interference filter (K-52) for K- or L-intermediate accumulation. After a single measurement, the film was illuminated at >600-nm (R-62 filter) for 1 min to recover the unphotolyzed dark-state of FR before proceeding to the next cycle of light-minus-dark measurement. Each measurement represents an accumulation of 128 interferograms measured before and after illumination at a resolution of 2 cm^{-1}, and each data represents an average of at least 20 measurements. The light-minus-dark difference spectra were calculated by subtraction of data collected before and after illumination.

Homology Modeling of FR

The structure used in this study was constructed using the SWISS-Model online server using the FR full length sequence as the target sequence and the XR structure from *Salinibacter ruber* (PDB: 3DDL) as the most suitable search template. This XR shares 34.13% sequence identity, a 0.37 similarity to the FR sequence as estimated by BLAST server, and yielded about 0.85 coverage.[32] The generated model has a QMEAN Z-score of -3.43 and a score of 0.45 for a model quality assessment as estimated by the QMEAN server.[33] The retinal and water molecules were

RSC Advances Accepted Manuscript

superimposed from the XR model and visualized using PyMol (PyMOL Molecular Graphics System).

RESULTS AND DISCUSSION

K- and L-like Intermediate State Formation in FR and the Correlation between UV-Visible and IR Ethylenic Modes

To further our understanding of the molecular mechanism underlying anion translocation in FR, we applied light-induced low-temperature UV-visible and FTIR difference spectroscopy for two trapped photoproducts: i) FR_K-minus-FR (K intermediate), and ii) $FR_{L'}$-minus-FR (L-like intermediate), as trapped at 77 K and 220 K, respectively (Fig. 2 and S4). We previously demonstrated that FR can be functionally expressed in *E. coli* and that it retains its function in liposomes.[18] The salt concentration used is 5 mM NaCl, which is expected to increase by ~100-fold in FR-liposome films.[28] The concentration dependency of UV-visible absorption spectra in solution (Fig. S2) at ambient temperature indicates a clear hypsochromic shift (blue-shift) with increased salt concentrations. The λ_{max} of hydrated films were estimated to be ≈520 nm (corresponding to ca. 0.5 M NaCl), as shown in Fig. 3a. We then monitored the light-induced FTIR difference spectra in H_2O-hydrated films illuminated with 520 nm light in the 77–240 K range (Fig. 2). The IR spectra show noticeable changes at the 1700–1520 cm^{-1} region and HOOP modes (970–950 cm^{-1}), with decreased intensity upon heating. The HOOP mode intensity is a good indicator for the decay of FR_K to subsequent state transitions.[29] As shown in Fig. 2, while the band intensity at 966 (+) cm^{-1} decreased significantly, a new one at 955 (+) cm^{-1} appears in the 200–220 K range, suggesting that the L-like state(s) is more prominent in this range, similar to other microbial rhodopsins, *e.g.*, HR and *Exiguobacterium sibiricum* rhodopsin (ESR).[29,34] However, residual contributions from a K-like state(s) should not be ruled out, and further specific analyses are required to dissect the individual contributions of different states in the 77–240 K range. We thus monitored the light-induced visible spectral changes in hydrated films illuminated with 520 nm light at 293 K, 220 K and 77 K (Fig. 3b). Spectral tuning (λ_{max} shifts) in retinal proteins can be attributed to several factors: i) the distortion in the polyene, ii) the changes in coulomb interaction between the protonated Schiff base (PSB) and its surrounding polar environment, and/or iii) the perturbations in the environment along the polyene chain.[1] Fig. 3b shows that both FR_K (77 K) and $FR_{L'}$ (220 K) are bathochromic states (red-shifted), with slight

RSC Advances Accepted Manuscript

spectral differences between them. This is different from the L-intermediate of HR (*e.g.*, N*p*HR), which exhibits a strong hypsochromic effect ($\Delta\lambda$ = 50 nm; ~0.24 eV),[20,34] suggesting different physical properties between FR and HR in the local environments of the retinal chromophore. Consistently, the data in Fig. 3c from the ethylenic stretching vibrations (νC=C) of the retinal in photoproducts formed at 77 K and 220 K at 1532 (+)/1540 (–) cm^{-1} and 1527 (+)/1538 (–) cm^{-1}, respectively, are bathochromic, whereas it upshifted in N*p*HR_K-minus-N*p*HR 1538 (+)/1527 (–) cm^{-1} recorded at 77 K.[22] The dissimilarity in the dark state (FR) at 77 K and 220 K could be a result of an additional minor component (λ_{max} = 529 nm) found in the dark state at 77 K (Fig. 3b). We assign the 1532 cm^{-1} (FR_K) and 1527 cm^{-1} ($FR_{L'}$) bands to the 13-*cis*,15-*anti* photo-isomerized retinal of FR_K, based on comparisons with previous reports in other rhodopsins.[22,31,35] We have previously shown that the light-adapted FR has ~13% 13-*cis* retinal (~10% increase from that of the dark-adapted FR), compared to 23% in N*p*HR_K.[18] It is worthwhile noting that the ethylenic modes of FR_K are well-resolved in comparison with that of the $FR_{L'}$ (the spectra at 1527 (+)/1538 (–) cm^{-1} in $FR_{L'}$ are normalized to ×2.1, Fig. 3c and S4).

Spectral changes in the retinal fingerprint vibrations upon photo-isomerization

The frequency region of 1290–1040 cm^{-1}, the fingerprint region, shown in Fig. 4 revealed similar features to other microbial rhodopsins.[27,31,36] This region in retinal proteins mostly assigned by Raman to the C–C stretching vibrations and the vinyl CCH rocking vibrations of the retinal polyene, whose kinetics coupling depends on the photoisomerization of the retinal, thereby providing useful information about its conformations.[36,37] The four negative bands at 1247 cm^{-1}, 1215 cm^{-1}, 1203 cm^{-1}, and 1166 cm^{-1} are possibly due to the predominant all-*trans*,15-*anti* retinal in the dark-state over 13-*cis* retinal forms.[34] The bands of the dark-state are surprisingly similar to that of the BR, a proton pump, of which the bands at 1255 cm^{-1}, 1216 cm^{-1}, 1203 cm^{-1}, and 1167 cm^{-1} were assigned to the C_{12}–C_{13}, C_8–C_9, C_{14}–C_{15} and C_{10}–C_{11} stretching vibrations, respectively.[27] The band at 1247 (–) cm^{-1} is likely a mix of C–C stretches and lysine rock (K246 in FR), and it is downshifted by 8 cm^{-1} from that of BR (1255 cm^{-1}).[36] This band is a good sign of dark-state recovery kinetics with all-*trans* retinal conformation, suggesting that the retinal conformation in the dark-state at 77 K resembles that of 220 K (1245 cm^{-1}) and that FR, like other retinal proteins, begins the photo-isomerization with a predominant all-*trans* retinal in the unphotolyzed state.[37] The fractional differences apparent in the dark state

RSC Advances Accepted Manuscript

between 77 K and 220 K (1213 cm^{-1}), especially the decrease in the intensity of band at 1215 cm^{-1} (dark state), could be due to the partial contribution of the temperature on the physical properties of FR in liposomes.[38] The positive peaks at 1191 cm^{-1}, 1186 cm^{-1}, and 1175 cm^{-1} are due to photo-isomerization of all-*trans* retinal before the onset of ion translocation. In proton pumps such as BR and ESR, only a single peak was found at 1194 cm^{-1} and assigned to a mixture of C–C stretches of the C_{10}–C_{11} and C_{14}–C_{15}, as inferred from FTIR difference spectra of isotopically labeled retinylidenes.[29,39] This peak likely corresponds to that found at 1191 cm^{-1} in FR_K, although in $FR_{L'}$, the peak intensity decreased at high-temperature and disappeared in D_2O exchanged FR, implying that it might not be solely originating from the photoproducts, at least in the FR case. Another possibility is that in D_2O the equilibrium between all-*trans*/13-*cis* retinal is slightly changed, or that the equilibrium between photoproducts of the all-*trans* photocycle could be changed, *i.e.*, a different mixture of intermediates is trapped at 77 K or 220 K during H_2O/D_2O exchange. This is reasonable since the dark-adapted FR samples contain ~3% of 13-*cis* retinal, which likely belongs to the 13-*cis*, 15-syn form.[18] The peak at 1186 (+) cm^{-1} is likely to have similar origin to that of 13-*cis* BR (1180 cm^{-1}).[31] The light-induced FTIR spectra of both FR_K and $FR_{L'}$ show an additional positive peak at 1178 cm^{-1} and 1175 cm^{-1}, respectively. This additional positive band (~1178 cm^{-1}) at the fingerprint region is unique to FR, although some microbial rhodopsins, such as ChR2 and *Anabaena* SR (ASR), exhibit positive bands at ~1175 cm^{-1} attributed to the all-*trans* retinal forms during the 13-*cis* photocycle.[40, 41] In the case of $FR_{L'}$, this peak exhibits a downshift of ~3 cm^{-1} with increased intensity. Overall, we conclude that the prominent retinal photoproducts of FR_K and $FR_{L'}$ are similar, a 13-*cis* retinal, with residual components of various all-*trans* forms. However, other experimental approaches need to be implemented to decisively resolve the individual photocycle components of each intermediate.

The assignment of HOOP wagging vibrations show that the retinal is more distorted in FR_K than in $FR_{L'}$

The retinal chromophore structure in microbial rhodopsins is well studied by Raman and IR spectroscopy combined with various isotope labeling.[37,39,40] The frequency region between 800–1040 cm^{-1} covers the HOOP wagging vibrations and the symmetric in-plane methyl rocking vibrations of the retinal chromophore (Fig. 5).[42,43] Therefore, the molecular vibrations in this

RSC Advances Accepted Manuscript

frequency region are good measures for the deviations in planarity of the polyene chain, *i.e.*, torsional deformations and distortions, as well as the changes in the retinal binding pocket.[27] The assignments of signals in this region are well documented from Raman and IR studies on archaeal and eubacterial rhodopsins.[31,42,43] The strong and H/D sensitive peak at 966 cm^{-1} in FR_K is due to C_{15}-HOOP vibration. In BR and H*s*HR, this peak appears at 974 cm^{-1} and 967 cm^{-1}, respectively (see Fig. S4 for N*p*HR HOOP mode).[34,36] The intensity of this peak decreased significantly in $FR_{L'}$ indicating that the retinal conformation in the FR_K intermediate is more distorted compared to $FR_{L'}$, which is a characteristic of a K intermediate in microbial rhodopsins.[29,44] This is supported by other experimental data and is consistent with theoretical data, indicating that the retinal conformation in the K state is more distorted than in KL-/L-intermediates.[27,44] The distortion in the retinal chromophore was suggested to facilitate the forward steps of the photocycle by storing energy low enough to prevent back-isomerization.[45] Additional positive peaks at 930 cm^{-1}, 903 cm^{-1}, 826 cm^{-1}, and 807 cm^{-1} were found in the FR_K and $FR_{L'}$, suggesting that factors affecting HOOP wags are not restricted to the RSB binding site but rather distributed along the polyene chain (Fig. 5). The band at ~800 cm^{-1} in HR, and 807 (+)/819 (–) cm^{-1} in FR_K- and $FR_{L'}$-minus-FR, was found to be indicative of the presence of 13-*cis* retinal based on Raman spectroscopy.[42] These bands exhibit a mild to moderate sensitivity to H/D exchange with ~5 cm^{-1} downshift with increased intensity at 807 cm^{-1} upon deuteration, whereas in the dark state it exhibits a decreased intensity when hydrated with D_2O (Fig. 5). The $FR_{L'}$ minus FR exhibits an additional positive peak at 843 cm^{-1}, which is insensitive to H/D exchange. Detailed assignments on HOOP wags of frequencies lower than 900 cm^{-1} have been studied in BR and SRII (also called *pharaonis* phoborhodopsin, *p*pR) using Raman and IR spectroscopy assisted by mutagenesis and isotope-labeled retinal.[42,43]

Interestingly, a highly symmetric peak to the C_{15}-HOOP vibration appeared at 950 (+) cm^{-1} in deuterated FR. No such change was noticed in BR or N*p*HR, but in BR, a positive peak in this frequency range (957 cm^{-1}) was assigned to the N−H vibration of the RSB. We are not able to assign this band based on previous reports because this band surprisingly appeared in the $FR_{L'}$ for both H_2O and D_2O hydrated FR (at 954 cm^{-1}), excluding the possibility that this peak purely originates from the N−H stretching vibrations of the RSB.[31] These differences in HOOP modes between FR_K and $FR_{L'}$ cannot be simply attributed to photo-isomerization, as other physical and chemical factors might have contributed to such changes. One explanation is that at high-

RSC Advances Accepted Manuscript

temperatures (220 K), the protein environment surrounding the retinal binding pocket is more relaxed compared to the lower-temperatures (77 K), potentially reducing the steric hindrance expected to affect the retinal binding pocket at 77 K, and increasing molecular motion.[43,46] However, previous FTIR studies in the HOOP mode of BR at ambient and cryogenic temperatures found no significant differences.[44,47] In the dark states of N*p*HR and BR, an H/D insensitive negative band appeared at 1007 cm^{-1} and 1009 cm^{-1}, respectively. These bands were found originate from in-plane methyl rocking vibrations of C_9 and C_{13} of the retinal polyene, as inferred from Resonance Raman (RR) and FTIR spectroscopy data.[34,37] A similar band at 1009 cm^{-1} in FR exhibits no change upon deuteration similar to observations in KR2, suggesting a different origin than the polyene in-plane methyl rocks.[31] The bands at 1030 (+)/ 1022 (–) cm^{-1} may also originate from the in-plane methyl rocks, as previously suggested for similar bands at 1024 (+)/ 1019 (–) cm^{-1} in BR.[36] In D_2O, a single positive band with low-intensity appeared only in the FR_K minus FR, whereas in the dark state, a slightly broader band at 993 cm^{-1} (up-shifted to 996 cm^{-1} at 220 K) appears, very similar to that of KR2 (at 991 cm^{-1}) in its Na^+ and H^+ pumping phases.[31] This band is strongly up-shifted compared to the 976 cm^{-1}(–) band of BR, which was assigned to the N–D in-plane rocking vibration, showing a dramatic downshift from its N–H in-plane rock that appears at ~1350 cm^{-1}.[36,48] The downshift in the N–D in-plane rock by ~17 cm^{-1} suggests a weaker deuterium bonding to the Schiff base nitrogen in FR compared to BR, pointing to a different environment between FR and BR in the RSB region. As compared to N*p*HR and KR2, an H/D exchange sensitive band at ~1038 cm^{-1} is in the dark-state of FR with similar property to those of N*p*HR and KR2, but different from BR, since this band does not appear in BR.[22,27,31] In *p*pR, a corresponding peak was found at 1041 cm^{-1} with H/D exchange as well as ^{15}N-Lys labelling sensitivity. Therefore, it was attributed to the C–N stretching vibration of K205 in *p*pR, corresponding to K246 in FR.[43] In FR_K and $FR_{L'}$, the corresponding peaks likely that appeared at ~1030 cm^{-1}, which is ~10 cm^{-1} downshifted from that of pR_K. Generally, as inferred from HOOP wags of both FR_K and $FR_{L'}$, the signal intensities of $FR_{L'}$ are significantly reduced in comparison with FR_K, suggesting a modified interaction between the PSB and the protein environment. Such modifications in interactions may facilitate the uptake of anions during the FR photocycle, a notion that was supported by the disappearance of FR_L in the anion-free photocycle.[18] Indeed, we previously showed that anion uptake is likely to take place in later photo-intermediates, possibly during the L/O and/or O transitions but not earlier.

RSC Advances Accepted Manuscript

The C=N stretching vibrations and the RSB hydrogen-bonding patterns during the photocycle

Fig. 6 shows the light-induced FTIR difference spectra of FR_K-minus-FR (top) and $FR_{L'}$-minus-FR (bottom) at the 1735–1560 cm^{-1} frequency region. The IR spectra in this frequency region are mostly attributed to the secondary structure of proteins (opsins) with some contributions from other groups.[27,49] The C=N stretching vibration of the Schiff base lies within the same range of the amide I frequency region, which has been well studied in other retinal proteins mainly by means of RR and IR spectroscopy.[27,37,40] The *ν*C=N-H of the RSB is highly informative with regards to the structure of the RSB binding pocket as well as the hydrogen-bonding of the PSB, which is a molecular determinant for the absorption maxima (λ_{max}) of retinal proteins.[50,51] The C=N-H and C=N-D bands have been studied intensively in BR, N*p*HR among other microbial rhodopsins.[22,50] Resolving the difference (isotope shifts) between the C=N-H and C=N-D stretches provides direct information about the strength of the hydrogen-bond of the RSB. In BR, the C=N-H stretching vibration is well-characterized and shows IR absorption at 1641 cm^{-1}, which undergoes a ~13 cm^{-1} downshift upon deuteration. This indicates strong hydrogen bonding for C=N-H in BR, whereas it only downshifts slightly (~2 cm^{-1}) in the K intermediate (BR_K).[27,52] The N*p*HR shows a corresponding peak in a lower frequency at 1634 cm^{-1} in H_2O with a downshift to 1621 cm^{-1} (~13 cm^{-1}) in D_2O, which is identical to that of BR, implying a similar hydrogen-bonding strength in the RSB (Fig. S4).[53] It should be noted that the spectral differences upon H/D exchanges are identical between BR and N*p*HR; however, the analyses of the ^{15}N-D Lys isotopes revealed an H-bond formation in BR,[50] whereas no H-bond is formed in N*p*HR.[22] By comparison, as shown in Fig. 6, FR exhibits a corresponding peak at 1628 cm^{-1} (same as SR-I), which downshifts to 1618 cm^{-1} in deuterium with a ~10 cm^{-1} difference, implying that the hydrogen-bonding in the RSB of FR is weaker than in N*p*HR. Upon FR_K and $FR_{L'}$ formation, the C=N-H stretch of both photo-products appears at 1618 cm^{-1}, although they differ in the degree of intrinsic bonding as could be inferred from the downshifts in the D_2O. In FR_K the spectrum downshifts with a ~10 cm^{-1}, whereas in $FR_{L'}$, it downshifts with ~6 cm^{-1}, indicating that the hydrogen bonding strength is weakened in $FR_{L'}$ but not broken. Previous IR experiments in HR_{La} and HR_{Lb} did not detect any signal corresponding to the C=N-H/-D stretches,[34] while RR data showed that the C=N stretch is upshifted to ~1640 cm^{-1} upon L

RSC Advances Accepted Manuscript

formation.[54] In this study, most of the spectral candidates for the C=N in the amide I region, except the one described above, exhibit only slight shifts upon deuteration, which might support the tentative assignment followed in this work. It can be concluded that the similarity between the BR (H^+ pump) and KR2 (Na^+/H^+ pump) Schiff base environments as inferred from their corresponding C=N stretches, regardless of the differences in amino acid residues in their local vicinities, extends the similarity between FR and N*p*HR in a similar way. These faces of comparison can be supported by previously reported data, indicating that in a functionally converted ClR (BR to HR analogs, BR-D85S), the C=N stretch downshifts to ~1632 cm^{-1} (H_2O) and ~1621 cm^{-1} (D_2O), similar to both N*p*HR and FR.[55] These lower frequencies in anion pumping rhodopsins might be a consequence of anion binding near the PSB, *i.e.*, attributable to electrostatic interactions in the local environment of the Schiff base.

Light-Induced Conformational Changes in the Apo-Protein upon the Formation of FR_K and FR_L, Intermediates

So far, there is no 3-D structural model for any eubacterial ClR that can be used to drive the interpretation of our spectroscopic data toward understanding the mechanism of anion translocation in FR. Therefore, we rely on our interpretation of the IR spectra on the homology model and associated multiple-sequence alignment with other microbial rhodopsins such as the XR, N*p*HR, BR and KR2, whose 3-D structures are available.[5,14,19,56] Fig. 6 includes the amide I frequency region (1700–1600 cm^{-1}), which is sensitive to the protein secondary structural components, mostly due to the C=O stretches in the protein moiety (coupled with the peptide bond N–H bending vibration), with contributions from the C=N and coupled N–H in-plane bends.[27,49] FR resembles N*p*HR in the photocycle.[18,21] Therefore, we compare the FR light-induced IR difference spectra obtained in this study with those of N*p*HR.[22] In the unphotolyzed state, FR (77 K) displays two prominent peaks at 1674 cm^{-1} and 1652 cm^{-1} with two minor components (low-intensity) at 1660 cm^{-1} and 1642 cm^{-1} at both sides of the major peak at 1652 cm^{-1} within the amide I region. In contrast to FR at 220 K, some structural changes in amide I are observed and can be summarized as follows: i) the prominent peak at 1652 cm^{-1} vanished, ii) the minor peak at 1660 cm^{-1} upshifted to 1663 cm^{-1} with a significant increase in intensity (×6), and iii) the broad peak at 1674 cm^{-1} significantly upshifted to 1684 cm^{-1}. The prominent peak at 1663 cm^{-1} at 220 K implies larger differences in the secondary structure between 77 K and 220

RSC Advances Accepted Manuscript

K, as this peak is a characteristic of the amide I region. Such structural changes in the unphotolyzed states of different temperatures were previously observed in N*p*HR at 170 K and 250 K, which were likely due to conformational changes in the protein moiety.[22] It is noteworthy that regardless of the significant differences in amino acid residues (10 out of 23 different residues are ~5 Å from the retinal) between FR and N*p*HR near the retinylidene binding pocket, FR displays similar FTIR difference spectra at 77 K. For example, N*p*HR exhibits negative prominent peaks at 1672 cm^{-1} and 1656 cm^{-1}, with minor peaks at 1645 cm^{-1} and 1694 cm^{-1} in the dark-state, which may correspond to the FR peaks at 1674 cm^{-1}, 1652 cm^{-1}, and 1642 cm^{-1}, respectively.[22,57] One obvious difference between FR and N*p*HR is that the peak at 1660 cm^{-1} displays a clear downshift upon deuteration to 1651 cm^{-1} (~ 9 cm^{-1}), which is not the case for the N*p*HR peak at 1656 cm^{-1} (Fig. S4). Such a shift is expected for C=N-H stretching vibrations of the arginine residue (guanidinium group) and/or the chromophore Schiff base, which absorb IR at this frequency range. The band pair at 1697 (–)/1690 (+) cm^{-1} in H*s*HR, corresponds to 1694 cm (–)/ 1688 (+) cm in N*p*HR, were previously assigned to the C=N-H^+ of R108 (R123 in N*p*HR) in helix-III, although this pair does not exhibit any spectral shifts in D_2O.[22,34] Therefore, the most likely candidate for the corresponding bands in FR at 1674 (–)/ 1686 (+) cm^{-1} and 1684 (–)/ 1690 (+) cm^{-1} for the FTIR difference spectra at 77 K and 220 K, respectively, is R107 (corresponds to R123 in N*p*HR and R82 in BR), although these bands are barely sensitive to deuteration. Another possible candidate is the *ν*C=O of asparagine residues, of which N110 (corresponding to T126 in N*p*HR) is more likely. Upon K formation (FR_K), FR displays peaks at 1686 cm^{-1}, 1664 cm^{-1}, 1645 cm^{-1}, 1635 cm^{-1}, and 1618 cm^{-1}, similar to those observed in N*p*HR_K. This likely means that FR involves similar changes in the protein backbone upon photo-activation.[34] All of these bands are upshifted upon L-like intermediate ($FR_{L'}$) formation by 1~6 cm^{-1}, except the band at 1618 cm^{-1}, suggesting even larger conformational changes in $FR_{L'}$ than in FR_K. The intense spectra at 1663 (–)/ 1649 (+) cm^{-1} in the L'-intermediate supports the above conclusion that FR undergoes larger conformational changes in the protein level upon L'-formation. It has also been shown that ChR2 (a popular optogenetics tool) exerts similar changes upon photo-activation at low temperature, as evidenced by the FTIR difference spectra at 1663 (–)/ 1648 (+) cm^{-1},[49,58] which is likely the case in FR. The analyses of amide II bands (1590–1565 cm^{-1} frequency) also reveal changes between these intermediates, as most of the bands at

RSC Advances Accepted Manuscript

this region are downshifted upon L'-formation, perhaps due to differences in the hydrogen bonding strengths between FR_K and $FR_{L'}$.

Hydrogen-bonding changes of carboxylates between FR_K and $FR_{L'}$

One of the major differences between archaeal and eubacterial ClRs is that the archaeal ClRs (*e.g.*, N*p*HR) possess at least one protonated carboxylate in its unphotolyzed state and in initial photoproducts (K- and L_a-intermediates), as inferred from the FTIR difference spectra at the 1760~1700 cm^{-1} frequency region. The absorption in this region is mostly due to the *ν*C=O of the protonated carboxylates of aspartate and glutamate, due to changes in their protonation states during the photocycle.[27,49,59] The H*s*HR, for instance, displays intense bands at 1744 (–)/ 1737 (+) cm^{-1}, which originate from the *ν*C=O of D141 (D115 in BR and D156 in N*p*HR).[34] The corresponding residue to D141 in FR is A144 of helix-IV, which may support the absence of a protonated carboxylate in FR during early stages of the photocycle (Fig. 6), even though FR has a carboxylate residue at position 242 (D242 in helix-VII, corresponding to D252 in N*p*HR and D212 in BR), near the RSB. Thus, we can safely conclude that D242 in FR and FR_K remains deprotonated during these states at a neutral pH (marine environment). At 220 K, shown in Fig. S5, FR displays bands at 1703 (–)/ 1715 (+) cm^{-1}, which undergo downshifts in D_2O up to 1699 (–)/ 1707 (+) cm^{-1}, suggesting a change in hydrogen-bonding of a protonated Asp and/or Glu upon $FR_{L'}$ formation, differing from FR_K. These low frequencies, however, are unusual and raise questions about their chemical nature; namely, whether they originate from the D242 in helix-VII or due to long-range perturbations in carboxylate residues upon photo-activation. One possible candidate of long-range carboxylates is E78 (corresponds to L85 in N*p*HR) in helix-II, which possibly forms an H-bond(s) with R107 near the extracellular side as deduced from the homology model. Such low frequencies were also observed in *Ca*ChR1 (channelrhodopsin-1) at a very similar frequency range, of which the bands were assigned to D299, corresponding to D242 in FR.[35]

Conclusion

In conclusion, we report the first FTIR spectroscopic analyses on the *Fulvimarina* rhodopsin (FR), a eubacterial chloride ion pumping rhodopsin. Two distinct photo-intermediates were trapped at 77 K and 220 K that are the K- and L'-intermediate states, respectively. We demonstrate that FR, as other microbial rhodopsins, undergoes photo-isomerization from an all-

RSC Advances Accepted Manuscript

trans to 13-*cis* upon photo-activation. The analyses show that the C=C ethylenic stretches of FR_K and $FR_{L'}$ are consistent with our previous flash photolysis study.[18] The data confirm that upon photo-activation, both K and L' intermediate states are red-shifted from the unphotolyzed state since our previous data revealed that FR_L (K/L and L/O) absorbs visible light maximally at 520~530 nm, in agreement with temperature dependent UV-visible spectra presented in this work. This finding also provides evidence for the agreement between $FR_{L'}$ and N*p*HR_L, regardless of the fact that N*p*HR_L is significantly blue-shifted at this state. Moreover, this study also demonstrates that FR undergoes various conformational changes in the protein moiety upon K- and L'-formation. In the case of $FR_{L'}$, these conformational changes likely include re-protonation of carboxylate residues. Finally, this paper provides further information about the differences between archaeal and eubacterial ClRs. Nonetheless, further studies are required to support the current findings, which might help in developing novel optogenetics tool.

Acknowledgments

The authors thank Rei Abe-Yoshizumi and Ito Shota for helpful discussion. F.H.M.K. is grateful to Nesreen I. Alsanousi (Osaka University) for technical support, and Jochen Zimmer and Sophia Lim (University of Virginia) for their critical reading of the manuscript. This work was supported by the Japanese Ministry of Education, Culture, Sports, Science, and Technology (Grant No. 25104009, H. K).

Abbreviations

AR-3, Archaeorhodopsin-3; ClR, chloride ion pumping rhodopsin; DOPC; 1,2-Dioleoyl-sn-glycero-3-phosphocholine; FR, *Fulvimarina* rhodopsin; H*s*HR, *Halobacterium salinarum* halorhodopsin; KR2, *Krokinobacter* rhodopsin-2; NaR, sodium ion pumping rhodopsin; N*p*HR, *Natronomonas pharaonis* halorhodopsin.

Notes and references

1 O. P. Ernst, D. T. Lodowski, M. Elstner, P. Hegemann, L. S. Brown and H. Kandori, *Chem. Rev.*, 2014, **114**, 126-163.

2 J. K. Lanyi, *Ann. Rev. Physiol.*, 2004, **66**, 665-688.

3 D. Oesterhelt and W. Stoeckening, *Proc. Natl. Acad. Sci. U. S. A.*, 1973, **70**, 2853-2857.

RSC Advances Accepted Manuscript

4 O. Beja, L. Aravind, E. V. Koonin, M. T. Suzuki, A. Hadd, L. P. Ngyuen, S. B. Jovanovich, C. M. Gates, R. A. Feldman, J. L. Spudich, E. N. Spudich and E. F. DeLong, *Science*, 2000, **289**, 1902-1906.

5 S. P. Balashov, E. S. Imasheva, V. A. Boichenko, J. Anton, J. M. Wang and J. K. Lanyi, *Science*, 2005, **309**, 2061-2064.

6 B. Schobert and L. K. Lanyi, *J. Biol. Chem*., 1982, **257**, 10306-10313.

7 M. Steiner and D. Oesterhelt, *EMBO J*., 1983, **2**, 1379-1385.

8 K. Inoue, H. Ono, R. Abe-Yoshizumi, S. Yoshizawa, H. Ito, K. Kogure and H. Kandori, *Nat. Commun*., 2013, **4**, 1678.

9 S. P. Balashov, E. S. Imasheva, A. K. Dioumaev, J. M. Wang, K. H. Jung and J. K. Lanyi, *Biochemistry*, 2014, **53**, 7549-7561.

10 R. A. Bogomolni and J. L. Spudich, *Proc. Natl. Acad. Sci. U. S. A.*, 1982, **79**, 6250-6254.

11 G. Nagel, D. Ollig, M. Fuhrmann, S. Kateriya, A. M. Musti, E. Bamberg and P. Hegemann, *Science*, 2002, **296**, 2395-2398.

12 G. Nagel, T. Szellas, W. Huhn, S. Kateriya, N. Adeishvili, P. Berthold, D. Ollig, P. Hegemann and E. Bamberg, *Proc. Natl. Acad. Sci. U. S. A.*, 2003, **100**, 13940-13945.

13 F. Zhang, J. Vierock, O. Yizhar, L. E. Fenno, S. Tsunoda, A. Kianianmomeni, M. Prigge, A. Berndt, J. Cushman, J. Polle, J. Magnuson, P. Hegemann and K. Deisseroth, *Cell*, 2011, **147**, 1447-1457.

14 H. E. Kato, K. Inoue, R. Abe-Yoshizumi, Y. Kato, H. Ono, M. Konno, S. Hososhima, T. Ishizuka, M. R. Hoque, H. Kunitomo, J. Ito, S. Yoshizawa, K. Yamashita, M. Takemoto, T. Nishizawa, R. Taniguchi, K. Kogure, A. D. Maturana, Y. Iino, H. Yawo, R. Ishitani, H. Kandori and O. Nureki, *Nature*, 2015, **521**, 48-53.

15 V. Gradinaru, M. Morgi, K. R. Thompson, J. M. Henderson and K. Deisseroth, *Science*, 2009, **324**, 354-359.

16 X. Han, B. Y., Chow, H. Zhou, N. C. Klapoetke, A. Chuong, R. Rajimehr, A. Yang, M. V. Baratta, J. Winkle, R. Desimone and E. S. Boyden, *Front. Syst. Neuosci*., 2011, **13**, 5:18.

17 S. Yoshizawa, Y. Kumagai, H. Kim, Y. Ogura, T. Hayashi, W. Iwasaki, E. F. DeLong and K. Kogure, *Proc. Natl. Acad. Sci. U. S. A.*, 2014, **111**, 6732-6737.

18 K. Inoue, F. H. M. Koua, Y. Kato, R. Abe-Yoshizumi and H. Kandori, *J. Phys. Chem. B*, 2014, **118**, 11190-11199.

19 M. Kolbe, H. Besir, L. O. Essen and D. Oesterhelt, *Science*, 2000, **288**, 1390-1396.

20 G. Varo, L. S. Brown, J. Sasaki, H. Kandori, A. Maeda, R. Needleman and J. K. Lanyi, *Biochemistry*, 1995, **34**, 14490-14499.

RSC Advances Accepted Manuscript

21 G. Varo, L. Zimanyi, F. Xiaolei, L. Sun, R. Needleman and J. K. Lanyi, *Biophys. J.*, 1995, **68**, 2062-2072.

22 M. Shibata, N. Muneda, T. Sasaki, K. Shimono, N. Kamo, M. Demura and H. Kandori, *Biochemistry*, 2005, **44**, 12279-12286.

23 A. K. Dioumaev and M. S. Braiman, *Photochem. Photobiol.*, 1997a, **66**, 755-763.

24 S. Gerscher, M. Mylrajan, P. Hildebrandt, M. -H. Baron, R. Muller and M. Engelhard, *Biochemistry*, 1997, **36**, 11012-11020.

25 M. S. Hutson, S. V. Shilov, R. Krebs and M. S. Braiman, *Biophys. J.*, 2001, **80**, 1452-1465.

26 C. Hackmann, J. Guijarro, I. Chizhov, M. Engelhard, C. Rodig and F. Siebert, *Biophys. J.*, 2001, **81**, 394-406.

27 A. Maeda, *Isr. J. Chem.*, 1995, **35**, 387-400.

28 Y. Furutani, K, Fujiwara, T. Kimura, T. Kikukawa, M. Demura and H. Kandori, *J. Phys. Chem. Lett.*, 2012, **3**, 2964-2969.

29 A. K. Dioumaev, L. E. Petrovskaya, J. M. Wang, S. P. Balashov, M. P. Kirpichnikov and J. K. Lanyi, *J. Phys. Chem. B*, 2013, **117**, 7235-7253.

30 A. K. Dioumaev and J. K. Lanyi, *Proc. Natl. Acad. Sci. U. S. A.*, 2007, **104**, 9621-9626.

31 H. Ono, K. Inoue, R. Abe-Yoshizumi and H. Kandori, *J. Phys. Chem. B*, 2014, **118**, 4784-4792.

32 K. Arnold, L. Bordoli, J. Kopp and T. Schwede, *Bioinformatics*, 2006, **22**, 195-201.

33 P. Benkert, M. Biasini and T, Schwede, *Bioinformatics*, 2011, **27**, 343-350.

34 Y. -S. Chon, H. Kandori, J. Sasaki, J. K. Lanyi, R. Needleman and A. Maeda, *Biochemistry*, 1999, **38**, 9449-9455.

35 J. I. Oregon, A. Yi, S. Mamaev, H. Li, J. Lugtenburg, W. J. DeGrip, J. L. Spudich and K. J. Rothschild, *Biochemistry*, 2015, **54**, 377-388.

36 S. O. Smith, M. S. Braiman, A. B. Mayers, J. A. Pardoen, J. M. L. Courtin, C. Winkel, J. Lungtenburg and R. A. Mathies, *J. Am. Chem. Soc.*, 1987, **109**, 3108-3125.

37 S. O. Smith, J. Lungtenburg and R. A. Mathies, *J. Membr. Biol.*, 1985, **85**, 95-109.

38 K. J. Rothschild, P. Roepe and J. Gillespie, *Biochim. Biophys. Acta*, 1984, **808**, 140-148.

39 K. Gerwert and F. Siebert, *EMBO J.*, 1986, **5**, 806-811.

40 V. A. Lorenz-Fonfria, T. Resler, N. Krause, M. Nack, M. Gossing, G. Fischer von Mollard, C. Bamann, E. Bamberg, R. Schlesinger and J. Heberle, *Proc. Natl. Acad. Sci. U. S. A.*, 2013, **110**, E1273-1281.

41 A. Kawanabe, Y. Furutani, K. –H. Jung and H. Kandori, *Biochemistry*, 2006, **45**, 4362-4370.

42 M. Braiman and R. Mathies, *Proc. Natl. Acad. Sci. U. S. A.*, 1982, **79**, 403-407.

RSC Advances Accepted Manuscript

43 Y. Furutani, Y. Sudo, A. Wada, M. Ito, K. Shimono, N. Kamo and H. Kandori, *Biochemistry*, 2006, **45**, 11836-11843.

44 A. K. Dioumaev, J. M. Wang and J. K. Lanyi, *J. Phys. Chem. B*, 2010, **114**, 2920-2931.

45 S. Hayashi, E. Tajkhorshid and K. Schulter, *Biophys. J.*, 2002, **83**, 1281-1297.

46 A. Maeda, M. A. Verhoeven, J. Lungtenburg, R. B. Gennis, S. P. Balashov and T. G. Ebrey, *J. Phys. Chem. B*, 2004, **108**, 1096-1101.

47 S. Smith, M. Braiman and R. Mathies, in *time-resolved vibrational spectroscopy*, ed. G. H. Atkinson, Academic Press, New York, 1983, pp. 219-229.

48 A. Maeda, J. Sasaki, J. M. Pfefferle, Y. Shichida and T. Yoshizawa, *Photochem. Photobiol.*, 1991, **54**, 911-921.

49 M. Nack, I. Radu, C. Bamann, E. Bamberg and J. Heberle, *FEBS Lett.*, 2009, **583**, 3676-3680.

50 H. Kandori, M. Belenky and J. Herzfeld, *Biochemistry*, 2002, **41**, 6026-6031.

51 H. S. Rodman-Gilson, B. Honig, A. Coteau, G. Zarrilli and K. Nakanishi, *Biophys. J.*, 1988, **53**, 261-269.

52 S. O. Smith, A. B. Mayers, J. A. Pardon, C. Winkel, P. P. J. Mulder, J. Lugntenburg and R. Mathies, *Proc. Natl. Acad. Sci. U. S. A.*, 1984, **81**, 2055-2059.

53 S. Gerscher, M. Mylrajan, P. Hildebrandt, M. Baron, R. Muller and M. Engelhard, *Biochemistry*, 1997, **36**, 11012-11020.

54 R. Diller, M. Stockburger, D. Oesterhelt, J. Tittor, *FEBS Lett.*, 1997, **217**, 297-304.

55 M. Shibata, K. Ihara and H. Kandori, *Biochemistry*, 2006, **45**, 10633-10640.

56 H. Luecke, B. Schobert, H. T. Richter, J. P. Cartailler and J. K. Lanyi, *J. Mol. Biol.*, 1999, **291**, 899-911.

57 C. Hackmann, J. Gaijarro, I. Chizhov, M. Engelhard, C. Rodig and F. Siebert, *Biophys. J.*, 2001, **81**, 394-406.

58 E. Ritter, K. Stehfest, A. Berndt, P. Hegemann and F. J. Bartl, *J. Biol. Chem.*, 2008, **283**, 35033-35041.

59 G. -J. Zhao and K. -L. Han, *Acc. Chem. Res.*, 2012, **45**, 404-413.

RSC Advances Accepted Manuscript

Figure Legends

Fig. 1. The architecture of the FR and retinal binding pocket. (a) An FR homology model depicts the chromophore binding pocket of FR with its characteristic NTQ motif, which is crucial for anion translocation through several defined photoreaction intermediates. Residues in parentheses are the TSA motif of HR. (b) The retinal photo-isomerization from all-*trans* to 13-*cis* in FR.

Fig. 2. Temperature-dependent light-induced FTIR difference spectra of FR hydrated film (1.0 µl H_2O). The light-induced difference FTIR spectra were recorded during heating from 77 K to 273 K with 30 min dark-adaptation before each measurement. Spectral rise and decay upon temperature increase are indicated on the 77 K and the 220 K difference spectra.

Fig. 3. (a) UV-visible absorption spectra of FR-liposome film hydrated with H_2O, and dark adapted for 15 min at 293 K, 220 K and 77 K, before measurement. (b) The light-minus-dark difference absorption spectra recorded at these temperatures. For each measurement, a hydrated film was illuminated with 520 nm light for 2 min followed by a recovery of unphotolyzed state by illumination with >600 nm light for 1 min and dark adaptation for 15 min at each temperature point. (c) Light-induced FTIR difference spectra of FR_K (red line), $FR_{L'}$ (blue line), and N*p*HR_K (grey line), measured at 77 K, 220 K, 77 K, respectively.

Fig. 4. Light-induced FTIR difference spectra magnified from spectra shown in Fig. S4 at frequency regions of 1290–1120 cm^{-1} of the retinal chromophore fingerprint.

Fig. 5. The HOOP vibrations of the retinal chromophore in the 1040–790 cm^{-1} frequency region. This frequency region is mostly attributable to the retinal chromophore distortion.

Fig. 6. Light-induced FTIR difference spectra at 1735–1560 cm^{-1} recorded at 77 K and 220 K for FR_K-minus-FR and $FR_{L'}$-minus-FR, respectively. Y-axis unit = 0.005 absorbance unit. Tentative C=N-H and C=N-D stretching vibrations in the FR_K-minus-FR and $FR_{L'}$-minus-FR are underlined.

RSC Advances Accepted Manuscript

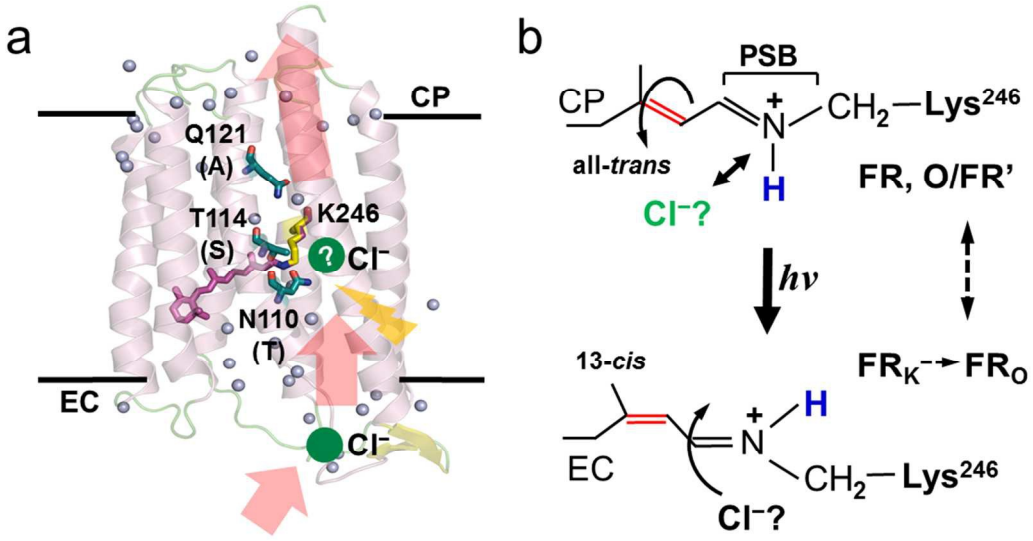

Fig. 1. Koua & Kandori

RSC Advances Accepted Manuscript

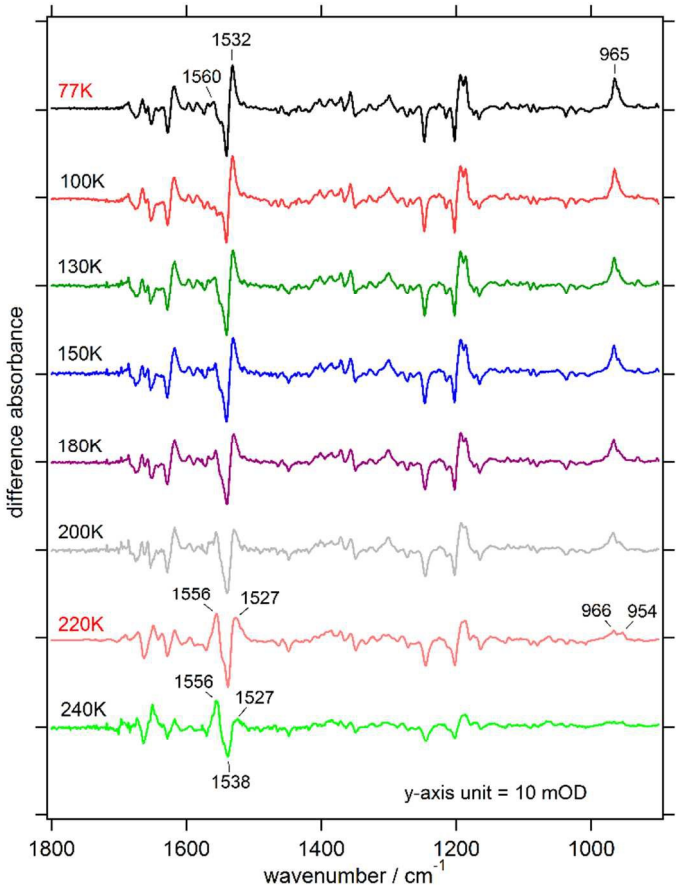

Fig. 2. Koua & Kandori

RSC Advances Accepted Manuscript

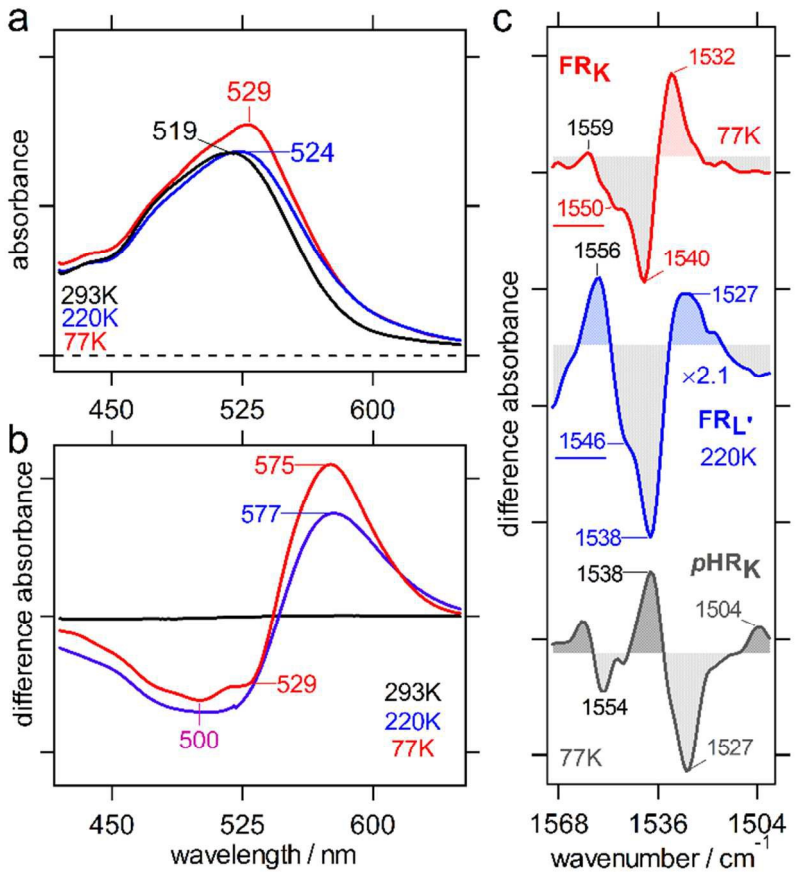

Fig. 3. Koua & Kandori

RSC Advances Accepted Manuscript

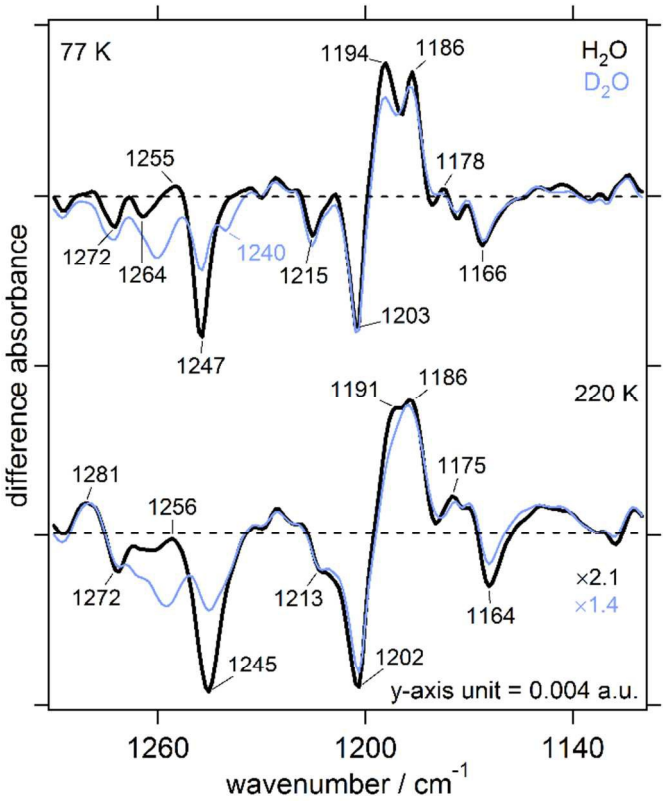

Fig. 4. Koua & Kandori

RSC Advances Accepted Manuscript

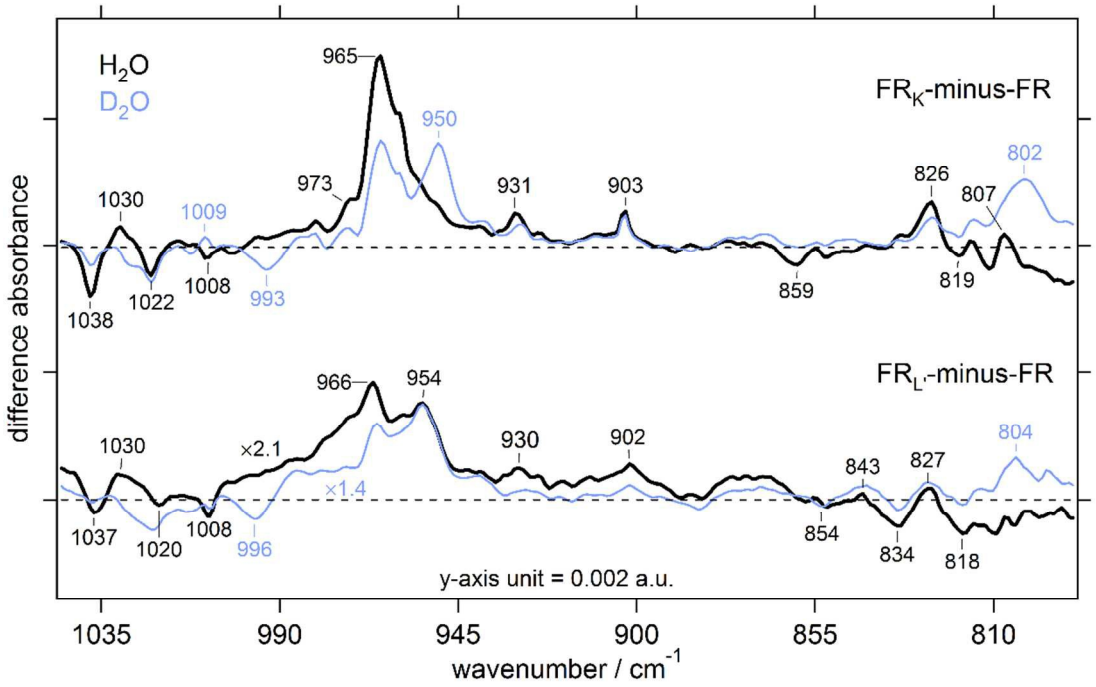

Fig. 5. Koua & Kandori

RSC Advances Accepted Manuscript

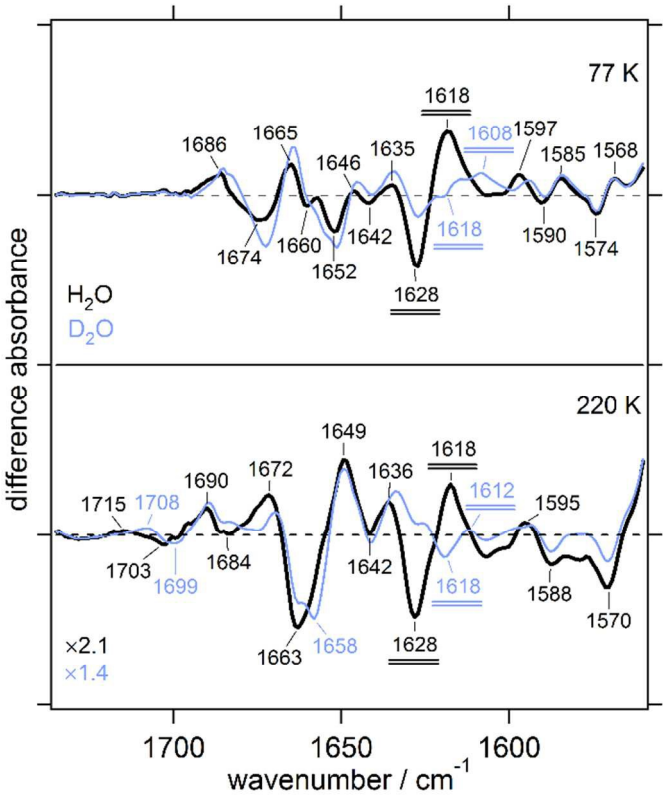

Fig. 6. Koua & Kandori

RSC Advances Accepted Manuscript

Table of Content Figure:

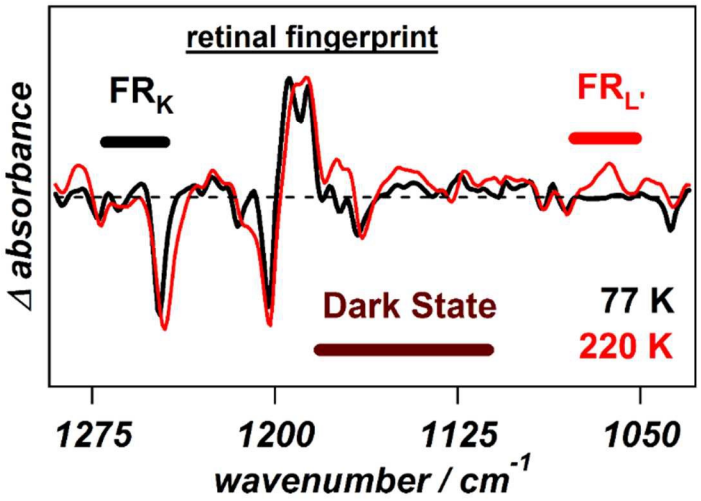

RSC Advances Accepted Manuscript